Journal of Magnetic Resonance 261 (2015) 73–82

Contents lists available at ScienceDirect

Journal of Magnetic Resonance

journal homepage: www.elsevier.com/locate/jmr

Spin polarization transfer mechanisms of SABRE: A magnetic field dependent study

Andrey N. Pravdivtsev [a,b], Konstantin L. Ivanov [a,b,*], Alexandra V. Yurkovskaya [a,b], Pavel A. Petrov [b,c], Hans-Heinrich Limbach [d], Robert Kaptein [e], Hans-Martin Vieth [a,f]

[a] International Tomography Center SB RAS, Institutskaya 3a, Novosibirsk 630090, Russia
[b] Novosibirsk State University, Pirogova 2, Novosibirsk 630090, Russia
[c] Nikolaev Institute of Inorganic Chemistry SB RAS, Acad. Lavrentiev Ave., 3, Novosibirsk 630090, Russia
[d] Institut für Chemie und Biochemie, Freie Universität Berlin, Takustr. 3, Berlin 14195, Germany
[e] Utrecht University, Bijvoet Center, Padualaan 8, NL-3584 CH Utrecht, The Netherlands
[f] Institut für Experimentalphysik, Freie Universität Berlin, Arnimallee 14, Berlin 14195, Germany

ARTICLE INFO

Article history:
Received 17 July 2015
Revised 5 October 2015

Keywords:
NMR
Spin hyperpolarization
Parahydrogen
SABRE
Level Anti-Crossings

ABSTRACT

We have investigated the magnetic field dependence of Signal Amplification By Reversible Exchange (SABRE) arising from binding of *para*-hydrogen (p-H_2) and a substrate to a suitable transition metal complex. The magnetic field dependence of the amplification of the ^{1}H Nuclear Magnetic Resonance (NMR) signals of the released substrates and dihydrogen, and the transient transition metal dihydride species shows characteristic patterns, which is explained using the theory presented here. The generation of SABRE is most efficient at low magnetic fields due to coherent spin mixing at nuclear spin Level Anti-Crossings (LACs) in the SABRE complexes. We studied two Ir-complexes and have shown that the presence of a ^{31}P atom in the SABRE complex doubles the number of LACs and, consequently, the number of peaks in the SABRE field dependence. Interestingly, the polarization of SABRE substrates is always accompanied by the *para*-to-*ortho* conversion in dihydride species that results in enhancement of the NMR signal of free (H_2) and catalyst-bound H_2 (Ir-HH). The field dependences of hyperpolarized H_2 and Ir-HH by means of SABRE are studied here, for the first time, in detail. The field dependences depend on the chemical shifts and coupling constants of Ir-HH, in which the polarization transfer takes place. A negative coupling constant of −7 Hz between the two chemically equivalent but magnetically inequivalent hydride nuclei is determined, which indicates that Ir-HH is a dihydride with an HH distance larger than 2 Å. Finally, the field dependence of SABRE at high fields as found earlier has been investigated and attributed to polarization transfer to the substrate by cross-relaxation. The present study provides further evidence for the key role of LACs in the formation of SABRE-derived polarization. Understanding the spin dynamics behind the SABRE method opens the way to optimizing its performance and overcoming the main limitation of NMR, its notoriously low sensitivity.

1. Introduction

Signal Amplification by Reversible Exchange (SABRE) is a variant of *Para*-Hydrogen Induced Polarization (PHIP) and a method to generate strong non-thermal nuclear spin polarization (called spin hyperpolarization) to enhance the Nuclear Magnetic Resonance (NMR) signal intensities of a substrate. The reactions that lead to SABRE are shown in Scheme 1 as described in Ref. [1]. In SABRE, a suitable transition metal catalyst dissolved in an organic solvent is used, which forms a complex with H_2 and a substrate [2] (although SABRE experiments in water are also feasible [3]). In the "reversible exchange stage" non-polarized H_2 is replaced by polarized *para*-H_2 (p-H_2, the H_2 molecule in its singlet nuclear spin state), which transfers its polarization to the liganded substrate. The mechanism of polarization formation in this process is also depicted in Scheme 1. Eventually the polarized substrate leaves the metal and joins a pool of free polarized substrate in solution. As long as p-H_2 is available this process can be repeated leading

Abbreviations: LAC, Level Anti-Crossing; MRI, Magnetic Resonance Imaging; NMR, Nuclear Magnetic Resonance; NSPD, Nuclear Spin Polarization Dispersion; o-H_2, *ortho*-H_2; p-H_2, *para*-H_2; PHIP, Para-Hydrogen Induced Polarization; Py, pyridine (aPy, axial Py; ePy, equatorial Py; fPy, free Py); SABRE, Signal Amplification By Reversible Exchange.

* Corresponding author at: International Tomography Center SB RAS, Institutskaya 3a, Novosibirsk 630090, Russia. Fax: +7 (383)3331399.
E-mail address: ivanov@tomo.nsc.ru (K.L. Ivanov).

http://dx.doi.org/10.1016/j.jmr.2015.10.006
1090-7807/

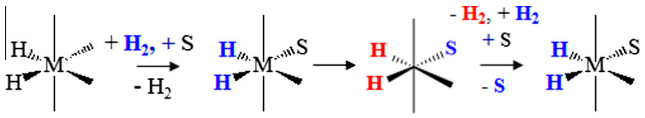

Scheme 1. Catalyzed SABRE polarization transfer from p-H_2 (H_2) to a substrate S according to Ref. [1] results in the formation of polarization of S and H_2. Here p-H_2 and o-H_2 are shown in bold face in blue and red, respectively; the hyperpolarized substrate molecule is shown in blue. (For interpretation of the references to color in this figure legend, the reader is referred to the web version of this article.)

to a substantial substrate polarization, which will survive until it decays by relaxation. Based on new experiments and computations discussed later, we clearly demonstrate that not only the substrate is polarized but the leaving dihydrogen exhibits an opposite polarization due to enrichment of *ortho*-H_2 (o-H_2, the triplet spin isomer). The SABRE process avoids hydrogenation of double or triple bonds by p-H_2 used in other versions of PHIP leading to consumption of the substrate. SABRE gets around the chemical conversion and can provide NMR signal enhancements up to four orders of magnitude. This technique has been used in mobile low-field Magnetic Resonance Imaging (MRI) [4], for NMR detection at nanomolar concentration [5,6] and for biomedical applications [7].

The key question in SABRE is the mechanism of spin transfer from p-H_2 to the substrate, see Scheme 1. An important related question is at what magnetic fields the SABRE-derived signal enhancements are the highest. With the aim to determine the SABRE field dependence (which we will call Nuclear Spin Polarization Dispersion, NSPD, by analogy with well-established relaxation studies) we have combined a p-H_2 bubbling device [8] with a field-cycling spectrometer, where the whole NMR probe can be shuttled between low and high fields [9]. Using this setup and exploiting the quantum–mechanical density matrix formalism, the SABRE polarization dispersion of Crabtree's catalyst (the description of SABRE catalysts is given below) was recently explored from an experimental and theoretical standpoint [10]. It was shown that the main parameters, which determine the polarization transfer at low magnetic fields, are the chemical shifts and scalar couplings of the active SABRE complex. The transfer occurs when spin functions of the same total spin mix at fields that correspond to so-called "Level Anti-Crossings (LACs)".

Despite the initial success in analyzing the SABRE field dependence by using the notion of LACs it is not clear whether this concept provides the general description of polarization transfer in field-dependent SABRE experiments. To confirm our expectations that polarization is transferred predominantly at LACs there is a need to collect the missing pieces of the puzzle in order to establish the complete description of the NSPDs. More specifically, the LAC-based description predicts strong effects of hetero-nuclei on the SABRE field dependence: the presence of a spin-1/2 hetero-nucleus is expected to double the number of relevant LACs and, consequently, the number of features in the SABRE field dependence. So far, SABRE field dependences have not been analyzed for ^{31}P-containing and phosphorus-free SABRE complexes under the same experimental conditions. In addition, the LAC-based coherent polarization transfer mechanism implies that polarization on the substrate is accompanied by a transition of H_2 from the NMR-silent *para*-state to an *ortho*-state giving observable magnetization of H_2. Indeed, Barskiy et al. [11] observed in the case of the Imes catalyst also hyperpolarized o-H_2. Polarized NMR signals coming from o-H_2 have also been found by Fekete et al. [12] but their origin was not discussed. Up to now, the H_2 polarization has not been analyzed systematically, most likely, because of experimental difficulties, namely, the short relaxation times of H_2 (~1 s). This inspired us to look closer at the H_2 polarization both experimentally and theoretically. Specifically, we study the polarization of the H_2-molecule and of the catalyst-bound dihydride, Ir-HH (cf. complexes **2** and **6** in Scheme 2), which is expected to have the same field dependence as the substrate, but is opposite in sign when the LAC-based mechanism is operative. Finally, with the aim to find out whether there are sizeable polarization transfer effects in other complexes we study the complete magnetic field dependence of SABRE.

Hence, to fill the missing gaps in the description of the SABRE effect and to obtain complete understanding of the underlying spin dynamics we perform here SABRE experiments at variable magnetic fields from 0.1 mT to 16.4 T for SABRE complexes, with and without the phosphorus atom. We also analyze the full NSPD of o-H_2; our setup enables measurements of the full NSPD curve even despite fast spin relaxation of H_2. The ultimate goal of our investigation is to show that LACs give the dominant contribution to SABRE and drastically simplify the analysis of NSPDs.

In general, analysis of the NSPD based on LACs not only provides a simple way to look at the complex spin dynamics in SABRE complexes but also enables (i) identifying active SABRE complexes and (ii) obtaining their NMR parameters, which are difficult to access by NMR experiments with thermally polarized spins. Notably, the values and signs of the scalar coupling between the hydride nuclei can be obtained, which, in turn, provide information on proton–proton distances [13] and can vary over a wide range [14–17]. Applications of LACs, for instance, for designing high-field SABRE experiments are also discussed in the paper.

2. Methods

2.1. Sample preparation

Presently, two SABRE catalysts are commonly used. One is [IrCl(COD)(Imes)] (**1**, Imes ≡ 1,3-bis(2,4,6-trimethylphenyl)imidazol-2-ylidene, COD ≡ cycloocta-1,5-diene), which forms the corresponding

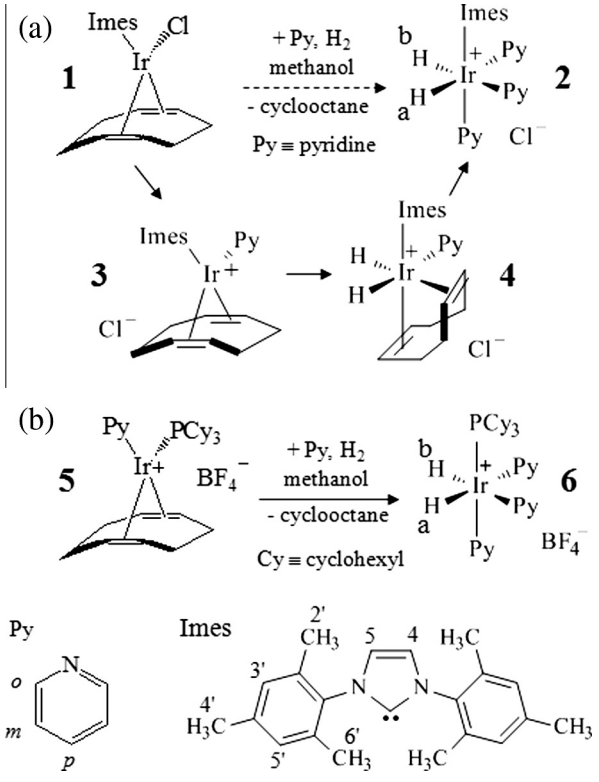

Scheme 2. (a) Formation of the Iridium dihydride **2** from the Iridium complex **1** with Imes ≡ 1,3-bis(2,4,6-trimethylphenyl)imidazol-2-ylidene as ligand *via* the intermediate complexes **3** and **4**. (b) Formation of the Iridium dihydride **6** from Crabtree's complex **5**. In both cases the cycloocta-1,5-diene ligand is released as hydrogenated species. Structures of pyridine (Py) and Imes are also shown. Ir-HH protons are indicated as Ha and Hb.

Iridium dihydride $[Ir(H)_2(Imes)(Py)_3]^+$ (**2**) with chlorine as counter-anion as depicted in Scheme 2a [18,19]. The second widely used catalyst is Crabtree's catalyst $[Ir(COD)(PCy_3)(Py)]^+BF_4^-$ (**5**, Cy ≡ cyclohexyl), which reacts with additional pyridine and dihydrogen to form the cationic Iridium dihydride $[Ir(H)_2(PCy_3)(Py)_3]^+$ (**6**, Py ≡ pyridine) as depicted in Scheme 2b, with BF_4^- as counter-anion [20]. The COD ligand is released by hydrogenation and replaced by pyridine [2,21–23]. This dihydride formation stage is then followed by the reversible exchange stage. Results of NMR studies of the complexes shown in Scheme 2 are presented in Supplementary Material (SM).

Crabtree's catalyst $[Ir(COD)(PCy_3)(Py)BF_4]$ **5** was purchased from ABCR, the carbene complex [IrCl(Imes)(COD)Cl] **1** was synthesized using a procedure described before [24]. The NMR solvents CD_3OD (99% D) and DMSO-d_6 were purchased from Deutero GmbH; the substrate Py was purchased from Sigma–Aldrich. All chemicals were used without additional purification. Solutions of pyridine and the pre-catalyst, **1** or **5** (4 mM, substrate/catalyst ratio 15:1), were prepared using CD_3OD as a solvent. For the preparation of p-H_2, we used a commercially available p-H_2 generator (Bruker) with an operating temperature of 32 K. The mixture enriched in the *para*-component (92% p-H_2 and 8% o-H_2) was kept in an aluminum bottle that was introduced into the employed gas bubbling system.

2.2. High-field NMR measurements

To reveal the structure of transient complexes in the associa tion–dissociation reactions of H_2 and ligands we performed NMR experiments using a Bruker high-resolution 700 MHz NMR spectrometer. To assign signals in the proton NMR spectra we applied the two-dimensional TOCSY technique [25]. Exchange between catalyst-bound Ir-HH and H_2 in solution was studied by the EXSY technique [26]. Experiments were done by using either thermally polarized H_2 gas or H_2 gas enriched in its *para*-component. To run the corresponding chemical reactions directly in the NMR sample tube we used the *in situ* bubbling device described previously [8]. The 1D spectra, TOCSY and EXSY spectra of Iridium complexes are shown in SM.

2.3. Field-dependent experiments

To perform SABRE experiments at variable magnetic field strength we made use of a fast field-cycling device, which utilizes transfer of the NMR probe with the sample in the inhomogeneous fringe field of a 7 T NMR magnet superimposed by the field from an additional coil system. Details of such experiments are outlined elsewhere [8,9]. Field-dependent experiments were performed in the following way. First the sample was moved to the polarization field of choice. At this field, the p-H_2 gas was bubbled through the sample during a fixed time period, typically between 10 and 30 s. When the gas flow was stopped the sample stayed for another 5 s at the polarization field; this time was needed to remove gas bubbles and to enable efficient polarization formation. Then the sample was moved back rapidly (in less than 0.4 s) to the observation field of the spectrometer and its NMR spectrum was obtained. In this fashion we performed measurements for polarization fields in the range from 0.1 mT up to 7 T. To extend the high field range we also performed measurements without field-cycling at other NMR spectrometers operating at 9.4 T (400 MHz for protons) and 16.4 T (700 MHz for protons) with the same bubbling times.

2.4. NMR enhancements

Enhancement factors were calculated in the following way. Thermally polarized NMR spectra were measured at $B_0 = 7$ Tesla prior to bubbling the sample with p-H_2. The integrated NMR signal intensities of substrates obtained in the low-field or high-field SABRE experiments were divided by their respective thermal signal intensities at 7 T giving the signal enhancement. In addition, we present the polarization in percent of maximum obtainable polarization. All NMR spectra shown here have been obtained with a single acquisition, the flip angle of the NMR pulses was set to either $\pi/4$ or $\pi/2$. The thermal polarization of H_2 in bulk solution and of Ir-HH in the SABRE complexes was measured at $B_0 = 7$ Tesla after 1 min of bubbling the sample with thermally polarized H_2 exhibiting a *para*-to-*ortho* ratio close to 1:3. The enhancement factor for H_2 and Ir-HH is the ratio of their hyperpolarized and their thermal signal intensities. In case of high-field SABRE (where the enhancements are lower than at low-field) we also subtracted the thermal polarization, *i.e.*, the signal obtained when the SABRE experiment was performed using normal H_2.

3. Theory

To unravel the complex spin dynamics at low field we performed an LAC analysis based on the premise that features in the SABRE field dependence can be assigned to particular LACs in the spin system.

As previously shown, [10] spin order transfer from bound polarized iridium dihydride spin pairs Ir-HH to the substrate is operative at fields where there is a crossing (*i.e.*, a degeneracy of energy levels) for pairs of spin states $|S,K\rangle$ and $|T_M,L\rangle$. Here, S and T_M (here $M = \pm, 0$) stand for the dihydride spin pair and K,L define the states of the substrate protons. When there is a perturbation, which mixes $|S,K\rangle$ and $|T_M,L\rangle$, the level crossing turns into an avoided crossing or LAC. This means that if the initial state is $|S,K\rangle$ after incorporation of p-H_2 according to Scheme 1, the spin function oscillates between $|S,K\rangle$ and $|T_M,L\rangle$. This implies that the chemical process is fast as compared to the spin dynamics. Then the Hamiltonian of the spin system experiences a sudden jump, which is a prerequisite for forming spin coherences. Thus, the bound substrate undergoes the transition $|K\rangle \rightarrow |L\rangle$; consequently, the state $|K\rangle$ becomes depleted and the state $|L\rangle$ becomes enriched, and thereby the substrate acquires hyperpolarization. For several simple spin systems it is possible to determine analytically the energy levels that have LACs and the corresponding magnetic fields. This allows one predicting the signs of polarization and the positions of peaks in the SABRE field dependence. This can be done, for instance, for an AA′B-system – a system composed of two 'isochronous' spins originating from p-H_2 (Ir-HH) and a third spin B, which belongs to the substrate. Typically, in SABRE complexes we have $\nu_A < \nu_B$ (here $\nu_{A,B}$ are the NMR frequencies of the A and B-spins) and $J_{AA'} < 0$. When $|J_{AA'}|$ is much larger than the other two couplings, J_{AB} and $J_{A'B}$, there is an LAC of the $|S\alpha\rangle$ and $|T_+\beta\rangle$ energy levels when [10,27,28]

$$\nu_A - \nu_B = J_{AA'} \tag{1}$$

That is, the LAC occurs at a magnetic field equal to $B_{LAC} = \left|\frac{2\pi J_{AA'}}{\gamma_p(\delta_A-\delta_B)}\right|$; here γ_p is the proton gyromagnetic ratio and δ_A, δ_B are the chemical shifts of the A- and B-spins, respectively. The other two couplings, J_{AB} and $J_{A'B}$, are responsible for the splitting of the $|S\alpha\rangle$ and $|T_+\beta\rangle$ energy levels at the crossing point, *i.e.*, they convert the level crossing into an LAC when $J_{AB} \neq J_{A'B}$. At a magnetic field where condition (1) is fulfilled transitions $|\alpha\rangle \rightarrow |\beta\rangle$ for the B-spin are expected; consequently, there will be a negative peak in its SABRE dispersion curve. For the AA′-protons *para*-to-*ortho* conversion occurs and the LAC will result in a positive peak in the H_2 and Ir-HH NSPD curves. Since there are no other LACs, there is only one such feature in the SABRE dispersion curve. When $\nu_A > \nu_B$ and $J_{AA'} > 0$ we obtain the same LAC and the same sign of polarization. When the sign of only one of the quantities, $(\nu_A - \nu_B)$ or $J_{AA'}$, changes we obtain an

LAC of $|S\beta\rangle$ and $|T_-\alpha\rangle$ and the sign of the polarization is positive for the B-spin and negative for the AA′-spins. Consequently, we obtain that

either (i) an LAC occurs between $S\alpha$ and $T_+\beta$ when $(\nu_A - \nu_B) = J_{AA'}$
or (ii) an LAC occurs between $S\beta$ and $T_-\alpha$ when $(\nu_A - \nu_B) = -J_{AA'}$

The presence of hetero-nuclei, notably ^{31}P, in the complex is of importance for SABRE because J-couplings to hetero-nuclei will double the number of LACs. In the simplest way this can be demonstrated for a four-spin AA′BP-system, where P is a spin-1/2 hetero-nucleus. If this spin has different couplings to the AA′-spins and the B-spin there will be the following crossings. The $|S\alpha, \pm\frac{1}{2}\rangle$ and $|T_+\beta, \pm\frac{1}{2}\rangle$ levels cross when [10]

$$\nu_A - \nu_B = J_{AA'} \pm (J_{AP} - J_{BP})I_z^P = J_{AA'} \pm \frac{J_{AP}}{2} \mp \frac{J_{BP}}{2} \quad (2)$$

In addition, there are crossings of the $|S\beta, \pm\frac{1}{2}\rangle$ and $|T_-\alpha, \pm\frac{1}{2}\rangle$ levels occurring when

$$\nu_A - \nu_B = -J_{AA'} \pm (J_{AP} - J_{BP})I_z^P = -J_{AA'} \pm \frac{J_{AP}}{2} \mp \frac{J_{BP}}{2} \quad (3)$$

Here $I_z^P = \pm\frac{1}{2}$ is the value of the z-projection of the P-nucleus. If $|J_{AP} - J_{BP}| > 2|J_{AA'}|$ (that is the case for Crabtree's catalyst) each of the equations gives one positive and one negative LAC field, but for our purpose only the positive fields have a physical reality. As a consequence, there are two relevant LACs, one resulting in negative polarization of the substrate (namely, the LACs of the $|S\alpha, \pm\frac{1}{2}\rangle$ and $|T_+\beta, \pm\frac{1}{2}\rangle$ states) and another one providing positive substrate polarization (namely, the LAC of $|S\beta, \pm\frac{1}{2}\rangle$ and $|T_+\alpha, \pm\frac{1}{2}\rangle$). One should note that in the case $|J_{AP} - J_{BP}| < 2|J_{AA'}|$ the LACs are also split but both features in the SABRE NSPD curve for the B-proton are expected to be negative, since one equation (2) predicts two positive field B_{LAC} positions, while Eq. (3) yields two negative B_{LAC} fields, which should be omitted. Thus, the bimodal 'positive–negative' shape of the SABRE NSPD curve is due to the relatively large J_{AP} coupling, as mentioned in our previous work [10]. For typical chemical shifts and spin–spin couplings all LACs and, consequently, all features in the SABRE NSPD curve are located at fields below 20–30 mT. Thus, the described LAC-based mechanism is expected to be operative at low magnetic fields. However, for very large couplings, *i.e.*, for those, which are typical for dihydrogen-like structures, the LACs can shift to much higher magnetic fields. Such couplings are known [29,30], for instance, for some metallic hydrides, reaching anomalous values, up to approximately 1500 Hz. Furthermore, J-couplings in complexes with dihydrogen (in which quantum rotation of dihydrogen persists) can reach very high numbers, up to 10^{12} Hz [17,31,32], which cannot be measured by traditional NMR spectroscopy. To find out whether complexes with such J-couplings contribute to the SABRE effect we will analyze the SABRE field dependence over an extended field range.

In order to visualize the action of LACs we have plotted in Fig. 1 schematically the energy level diagram of an AA'B system of spins 1/2 as a function of the magnetic field [33,34]. In SABRE experiments, initially, only the spin states $|S\beta\rangle$ and $|S\alpha\rangle$ are populated. Outside an LAC the spin functions and their population will not change as long as relaxation is neglected and the complex is stable. As illustrated in Fig. 1, for most magnetic field values the spin eigen-functions can well be approximated in terms of products of the "strong coupling" spin functions $|S\rangle$ or $|T_M\rangle$ of H_2 and $|\alpha\rangle$ or $|\beta\rangle$ of the substrate spin. When the energies of two levels approach each other and there is interaction between them, they would repel each other. In one of the two spin manifolds shown in Fig. 1 there is an LAC. The interaction at the LAC depends on the values of the J-coupling constants. Note that there is also an LAC exactly at zero field, which is, however, unimportant in SABRE

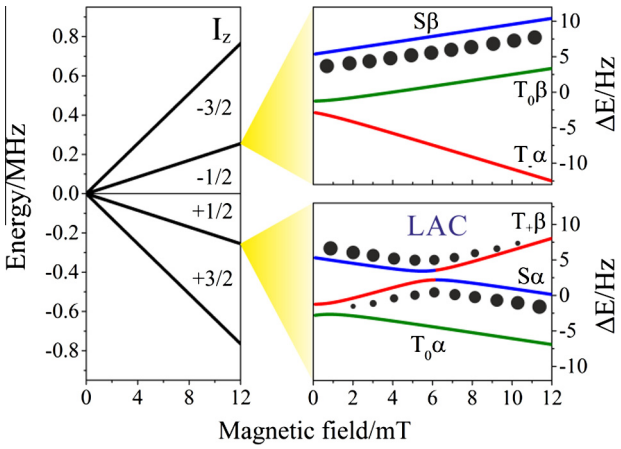

Fig. 1. Scheme demonstrating the role of LACs in SABRE formation. Here we show the energy levels of an AA′B-system as functions of the external magnetic field. In the left panel, we show energies of nuclear spin sub-ensembles with different projection, I_z, of the total spin; in the right panel we zoom into the spin manifolds I_z equal to −1/2 (top) and +1/2 (bottom). In this example there is an LAC of the $|S\alpha\rangle$ and $|T_+\beta\rangle$ states resulting in mixing of their populations; in the other spin manifold there is no LAC and, consequently, no efficient polarization transfer pathway. Here the energy of the singlet states, T_0-states and $T_\pm$-states is shown in blue, green and red, respectively. State populations resulting from the singlet-state preparation of the AA′-spins at different field positions are schematically shown by balls. The size of the balls for each state $|i\rangle$ corresponds to its population, given by the square of the mixing coefficient, $|\langle i|S\beta\rangle|^2$ (for the upper graph) and $|\langle i|S\alpha\rangle|^2$ (for the lower graph). At the LAC population is evenly mixed between the $|S\alpha\rangle$ and $|T_+\beta\rangle$ levels resulting in flips of the B-spin, $|\alpha\rangle \rightarrow |\beta\rangle$. Calculation parameters: chemical shift difference is $\delta_A - \delta_B = -30$ ppm; J-couplings are $J_{AA'} = -7$ Hz; $J_{AB} = 2$ Hz, $J_{A'B} = 0$. To visualize the energy levels better, in the right panels, for each manifold we have subtracted the large Zeeman energy, ν_{avg}, from the actual energy and show the energy difference ΔE. (For interpretation of the references to color in this figure legend, the reader is referred to the web version of this article.)

experiments presented here (although it is relevant for zero-field SABRE experiments, see, for instance, Ref. [35]).

Finally, let us stress that the LAC analysis always predicts polarization of the AA′-protons (which stand here for Ir-HH) of the same amplitude and opposite sign as compared to the B-proton. The explanation for this fact is that (i) we start with zero net polarization and that (ii) the two groups of spins, the AA′-protons and the B-proton, are polarized together in the same process. Since the spin Hamiltonian of the scalar coupled spin system conserves the z-projection of the total spin of the complex, the resulting net polarization (the sum of the polarizations of the AA′-protons and the B-proton) stays equal to zero. Indeed, if we consider, for instance, the LAC of the $S\alpha$ and $T_+\beta$ levels, we obtain $\alpha \rightarrow \beta$ transitions resulting in negative polarization of the B-spin and $S \rightarrow T_+$ transitions, which yield positive polarization of the AA′-spins of the same size. Thus, H_2 goes from the NMR-silent *para*-state to one of the triplet states, *i.e.*, to an *ortho*-state. As we show below, this simple consideration indeed explains SABRE effects for two different forms of H_2: at LACs hyper-polarized *o*-H_2 is formed with strongly enhanced NMR signals.

To complement our LAC analysis we performed numerical calculations of hyperpolarization as a function of the magnetic field, which were done according to the method described in Ref. [10]. We assumed that at low field the mechanism of spin-order transfer from *p*-H_2 to the substrate is purely coherent; all relaxation effects were neglected. For these calculations we used the sets of chemical shifts and J-couplings in the complex and in the substrate as input parameters. Chemical shifts of protons in the SABRE complexes were determined from NMR spectra. For the bound substrates we used the same values for the J-couplings as for the free substrate molecules. For the couplings between Ir-HH and substrate we assumed small values of less than 3 Hz; their exact values are

not important for our analysis. The coupling between the Ir-HH protons was a free parameter; as we show below, it is about −7 Hz. The simulation parameters are given in SM. The calculated NSPD curves were always scaled to the experimental data.

A more general theoretical approach to SABRE should explicitly take into account not only spin mixing but also chemical exchange and relaxation processes. A relatively simple phenomenological way how to do this has been proposed by Adams et al. [36] and by Hövener et al. [37]; a more rigorous approach [14] to PHIP in the presence of exchange is provided by the Alexander–Binsch theory [38,39]. However, performing such an extension of the theory is a separate task, which is out of the scope of the present work.

4. Results

To assign signals in SABRE spectra we performed a systematic NMR study of the complexes, shown in Scheme 2. One-dimensional NMR spectra and two-dimensional TOCSY spectra used for assigning the proton signals are shown in SM. In the spectra of complexes **2** and **6** there are signals from three forms of Py present in SABRE experiments: free Py in solution, hereafter denoted as fPy, and Py molecules bound to the complex as equatorial and axial ligands, denoted as ePy and aPy, respectively. Each of the Py species has NMR lines corresponding to its *ortho*-, *para*- and *meta*-protons. In addition, we observe polarized signals coming from H_2 dissolved in methanol and Ir-HH (see below).

The two hydrogen positions H_2 and Ir-HH undergo exchange, which is demonstrated by EXSY experiments performed for complex **2** and complex **6**, see SM. The existence of the EXSY cross-peaks is a clear indication of exchange between Ir-HH and free H_2, and between Ir-HD and free HD. Such an exchange is observed for both catalysts. The presence of signals coming from Ir-HD and HD is tentatively explained here by H–D exchange in the H_2 molecule occurring in the following reaction:

$$CD_3OD + \text{Ir-HH} \rightarrow CD_3OH + \text{Ir-HD} \quad (4)$$

Methanol-d_4 is the only source of deuterons and can be coordinated by iridium. Our results are in contradiction with a conclusion made in Ref. [11] where it is claimed that deuterons come only from deuterated pyridine; H–D exchange in various complexes has also been described by Glöggler et al. [40].

To study the SABRE field dependence we performed experiments with *p*-H_2 instead of H_2. A typical SABRE spectrum for the Imes catalyst at low fields is shown in Fig. 2. Here polarization is formed at magnetic fields of about 3–15 mT. Strongly polarized signals from Py are observed, which are always negative. In addition, the lines of free H_2 and Ir-HH are polarized with their polarization phase opposite to that of Py, *i.e.* positive, as predicted by the LAC analysis (see Section 5).

When Crabtree's catalyst is used, one can also clearly see the low-field SABRE effect, see Fig. 3: spin order transfer is efficient

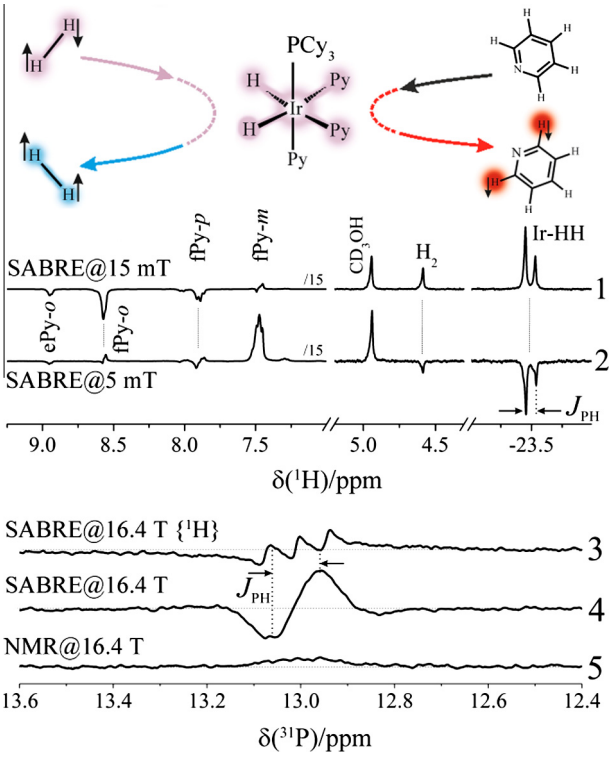

Fig. 3. (1 and 2) ^{1}H SABRE spectra of the sample containing 60 mM Py and 4 mM of Crabtree's catalyst **1** in CD_3OD obtained after bubbling *p*-H_2 at 5 mT (spectrum 1) and 15 mT (spectrum 2); the spectra were taken at 300 MHz with a $\pi/4$ pulse; signals of Py, H_2 and Ir-HH are indicated. Signals of H_2 and Ir-HH are enlarged for clarity. (3 and 4) ^{31}P SABRE spectra taken at 16.4 T. The SABRE experiment is run at 16.4 T after bubbling *p*-H_2 for 30 s. Here we show the ^{31}P spectrum with decoupling of the aliphatic protons (spectrum 3) and without decoupling (spectrum 4); the thermal ^{31}P NMR spectrum is shown for comparison (spectrum 5). The ^{1}H–^{31}P coupling, J_{PH} of 23.4 Hz, is indicated in the ^{1}H and ^{31}P spectra.

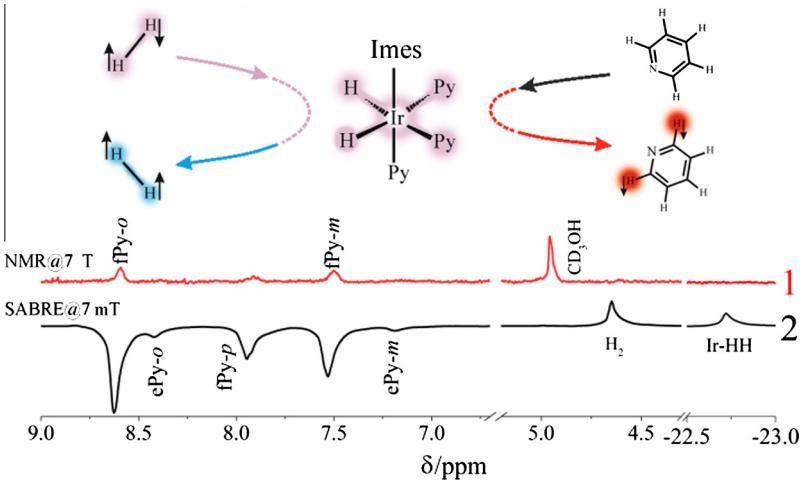

Fig. 2. Thermal NMR spectrum of complex **2** at 7 T (enlarged by a factor of 200, spectrum 1) and SABRE spectrum obtained after polarization preparation at 7 mT (spectrum 2). Signal assignment is given in the spectra.

at magnetic fields in the range 3–20 mT. As in the previous case, one can see the SABRE effect of H_2 and Ir-HH; again, the sign of the H_2 polarization is opposite to that of Py. In contrast to the Imes case, the sign of polarization of Py can be positive or negative (examples for both cases are shown in Fig. 3). Interestingly, in Crabtree's catalyst one can observe spin hyperpolarization not only for protons but also for the ^{31}P nucleus, which is present in the active complex, see Fig. 3 (traces 3 and 4). The SABRE-derived polarization of phosphorus is considerably stronger than the thermal polarization; its anti-phase character clearly indicates that it is formed by transfer from *p*-H_2. This observation together with the presence of considerable proton–phosphorus coupling (indicated in Fig. 3) shows that the ^{31}P atom is involved in the spin evolution in the SABRE experiments. In a recent work by Zhivonitko et al. [41] SABRE-like effects on ^{31}P have also been demonstrated. As we show below, not only do protons affect the polarization of the phosphorus atom but the presence of the ^{31}P atom has also a significant influence on the SABRE NSPD curve and the polarization of protons at low fields.

We also measured the full dispersion curve of the SABRE-derived polarization for both catalysts. Here, we focus mainly on the low-field part, which is conditioned predominantly by LACs (as discussed in Section 3 and demonstrated below), and then briefly present results for high fields.

The results for the Imes catalyst are presented in Fig. 4. In full accordance with the LAC-based theoretical predictions for the field dependence there is single negative peak observed, see Fig. 4a. We attribute this peak to the LAC that occurs when the difference in the Zeeman interactions of the Ir-HH and ePy-protons is approximately equal to the J-coupling between the Ir-HH protons. The polarization sign is negative, which is also consistent with the LAC analysis.

As predicted, the dispersion curve of both H_2 and Ir-HH exhibits exactly the opposite behavior regarding amplitude and sign of the polarization, see Fig. 4b. The explanation for this observation is that first Ir-HH and bound Py are polarized together in the complex and then polarization is transferred from bound Py to fPy and from Ir-HH to free H_2 in the solvent by means of chemical exchange (the presence of this exchange process is revealed by the EXSY experiment presented in SM). The opposite sign of polarization of Py and Ir-HH is explained in Section 3.

It is worth noting that the experimental curves and the simulations are in very good agreement. For instance, we can reproduce the experimentally observed differences in polarization of individual protons of Py, see Fig. 4c. Only the *ortho*-protons of Py (the ones, which have sizable couplings to the Ir-HH protons in the SABRE complex) are polarized directly from *p*-H_2, whereas the other protons acquire polarization indirectly in the course of its re-distribution in the Py molecule due to their J-coupling with *ortho*-protons. The exact behavior of polarization in such a system is relatively complex and can be analyzed only numerically [42,43]. Clearly, our model provides an appropriate description of polarization transfer within the spin system of Py.

When the phosphorus-containing Crabtree's catalyst is used, the SABRE NSPD curve has two peaks: a positive and a negative one, see Fig. 5a. This is in full agreement with the LAC analysis: the presence of a spin-1/2 hetero-nucleus doubles the number of LACs and, consequently, the number of the features in the SABRE NSPD curve. Qualitatively the same behavior was found [44] for a set of other N-containing substrates. These observations demonstrate the significant role of spin-1/2 hetero-nuclei in the formation of SABRE at low fields.

Again, the polarization of H_2 behaves in exactly the opposite way as compared to that of the substrate (compare Fig. 5a and b). The explanations of this observation and of the

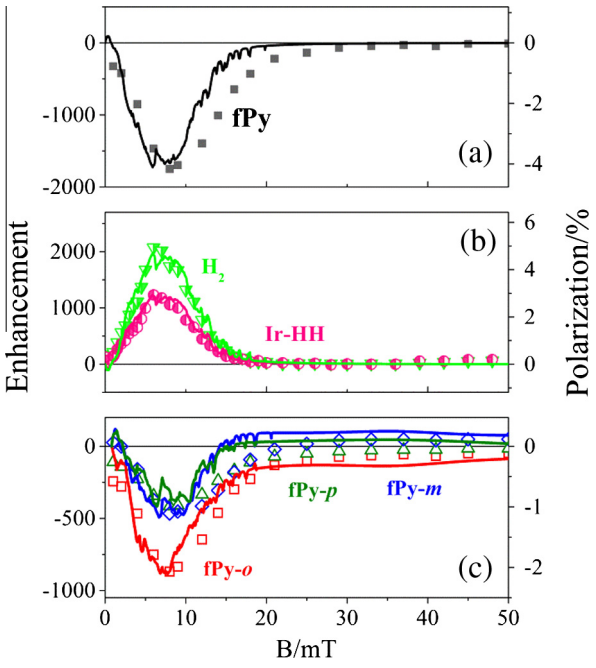

Fig. 4. Field dependence of the SABRE effect for Py obtained using the Imes-complex. Total net polarization of Py (full squares) is shown in subplot (a); signals of H_2 (green triangles) and Ir-HH (pink circles) are shown in subplot (b). Signals of the *ortho*- (squares), *meta*- (diamonds) and *para*- (triangles) protons of Py are shown in subplot (c). Solid lines show the calculation results for coherent polarization transfer in the SABRE complex at low fields. (For interpretation of the references to color in this figure legend, the reader is referred to the web version of this article.)

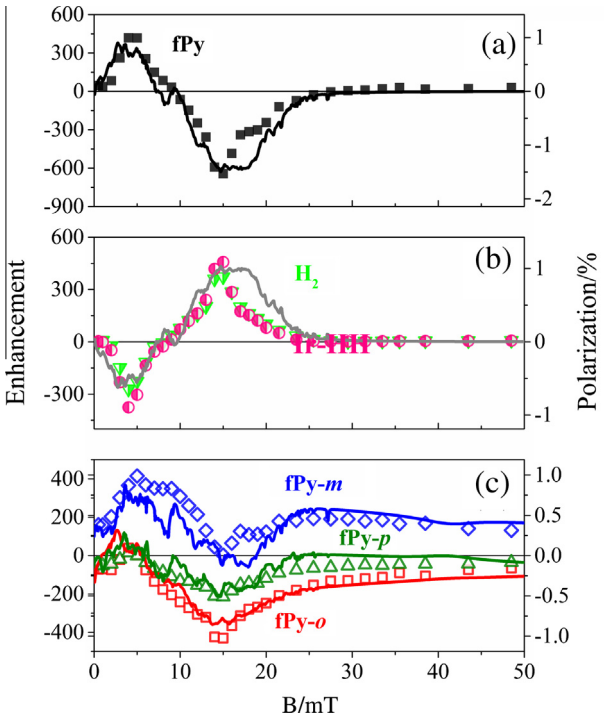

Fig. 5. Field dependence of the SABRE effect for Py obtained using Crabtree's catalyst. Total net polarization of Py (full squares) is shown in subplot (a); signals of H_2 (green triangles) and Ir-HH (pink circles) and are shown in subplot (b). Signals of the *ortho*- (squares), *meta*- (diamonds) and *para*- (triangles) protons of Py are shown in subplot (c). Solid lines show the calculation results for coherent polarization transfer in the SABRE complex at low fields. (For interpretation of the references to color in this figure legend, the reader is referred to the web version of this article.)

intensity differences between protons (Fig. 5c) are the same as in the case of the Imes catalyst.

One should also note that the different behavior of different Py protons (see Fig. 5c) is again well reproduced by the calculation.

Hence, the results shown in Figs. 4 and 5 demonstrate that although the simple formulas obtained earlier for LACs [10] in model systems of only a few spins cannot provide exact results for real systems (up to 15 protons for three Py's in complexes **2** and **6**) they properly reproduce the field range for LACs and predict the polarization sign. Thus, LACs well account for the low-field SABRE dispersion curves in spin systems observed so far.

Finally, we emphasize that another contribution to SABRE is given by cross-relaxation. We anticipate that this contribution is minor and thus of no relevance when coherent LAC-based transfer mechanisms are operative; however, in a field range without LACs cross-relaxation can be predominant. This is the case at high fields, where SABRE-derived NMR enhancements have been recently reported [11]. To gain additional insight into the SABRE mechanism and its field dependence we have also obtained data in an extended field range, up to 16.4 T, for the Imes system with Py used as a substrate, see Fig. 6. At magnetic fields above 2 T we have observed sizeable SABRE effects; these results are in agreement with those reported earlier, which were attributed to polarization transfer by cross-relaxation [11]. In contrast, when using Crabtree's catalyst we did not detect any considerable high-field SABRE effect.

5. Discussion

The results of our *p*-H_2 induced substrate polarization experiments at variable field and their theoretical analysis described above corroborate our previous proposal that low-field SABRE is caused by the presence of LACs in transition metal dihydrides formed from *p*-H_2 and substrate molecules such as pyridine. In addition to this result, in this section we would like to address several issues that emerge from our observations. Specifically, we dwell on (i) the information that can be extracted from modeling NSPD curves, (ii) polarization of the H_2 species and (iii) high-field SABRE.

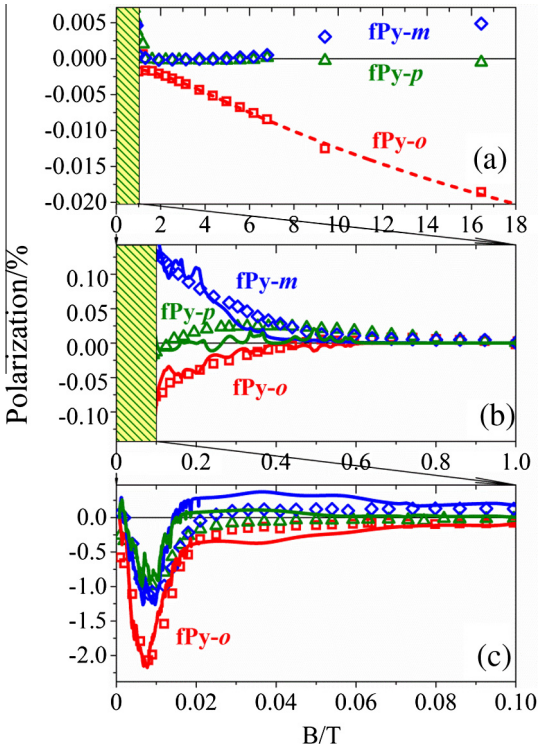

Fig. 6. Complete dispersion curve of the SABRE effect for Py obtained using the Imes catalyst shown for the field range 1.5–16.4 T (a), 0.1–0.7 T (b) and 0–0.1 T (c). Here signals of the *ortho*- (squares), *meta*- (diamonds) and *para*- (triangles) protons of Py are shown. Note the different vertical scales. Solid lines show the calculation results for coherent polarization transfer in the SABRE complex at low fields; the high-field SABRE data were modeled only for the *ortho*-protons assuming the cross-relaxation mechanism of polarization transfer (dashed line).

5.1. Simulation of the field dependence of substrate SABRE at low magnetic fields

The curves describing the field-dependent substrate SABRE at low fields depicted in Figs. 4 and 5 were calculated using the theory described previously [10] (*cf.* Section 3). As stated above, polarization transfer from the dihydride nuclei to the substrate nuclei is a coherent mixing process mediated by scalar magnetic couplings, but not by cross-relaxation. The agreement between experimental and calculated curves is very good in spite of a number of simplifying assumptions made. Thus, it was assumed that (i) the polarization transfer takes place in the dihydrides according to Scheme 1; (ii) that hydrogen and substrate ligand exchange rates and T_1-relaxation determine only the magnitude but not the shape of the curves: their effect can be taken into account by using a different empirical fitting constant for vertical scaling of each curve; and (iii) that only polarization transfer to a single substrate molecule needs to be considered. In this way, all systems studied could be treated with a computer program, which takes into account a large number of coupled spins.

The question then arises what we can learn from these simulations. The main information is that the polarization transfer really takes place in the dihydride state as depicted in Scheme 1. This results from the finding that the coupling constant $J_{AA'}$ between the two dihydride nuclei is negative and of the order of −7 Hz. As discussed in the previous section, the negative sign of $J_{AA'}$ is the reason why the substrate enhancements are all negative in the absence of coupling to a phosphorus nuclei, whereas the enhancement of the free dihydrogen is positive, as depicted in Fig. 4 for **2**. The presence of the coupling to the ^{31}P atom, which is about 23 Hz, in the case of **6** leads to two broad peaks of opposite signs as illustrated in Fig. 5. These features demonstrate the dominance of the couplings for the shape of the enhancement curves.

Let us now come back to the negative sign of the couplings between the two dihydride nuclei. As has been shown previously [13], as long as so-called "exchange couplings" which are all positive are absent, the "magnetic" coupling constant $J_{AA'}$ correlates with the HH distance. If the distance is smaller than 2 Å, the coupling is positive, but becomes negative at distances above 2 Å. A value of −6 to −7 Hz corresponds then to a proton–proton distance in Ir-HH of about 2.3 Å. This value corresponds clearly to a dihydride.

Polarization transfer from the dihydride nuclei to the bound substrate takes place *via* coupling constants between Ir-HH and the substrate protons. We are not able to assess their values by NMR spectroscopy, but determine them by modeling SABRE field dependences: this provides couplings of about 1–3 Hz, apparently sufficient to promote polarization transfer within the lifetime of the dihydrides. However, taking into account chemical exchange and relaxation may give a better accuracy in determining these J-coupling constants.

The generality of the LAC concept as applied to SABRE at low fields (where relaxation effects are not relevant) can be demonstrated by analyzing the data for other SABRE substrates. For instance, the prediction of bimodal SABRE field dependences for complexes with ^{31}P bound to the metal and unimodal dependences if phosphorus is absent is indeed borne out by the SABRE results of

Dücker et al. [44] for a variety of substrates with Crabtree's catalyst and by Zeng et al. [45] for a several substrates with the Imes complex. We also obtained similar data sets for several other substrates, which confirm the general behavior predicted by the LAC-analysis: the NSPD is unimodal or bimodal for the complexes without and with the ^{31}P atom (these data will be published elsewhere).

5.2. Polarization of o-H_2

By analyzing the full SABRE field dependence for all NMR signals we can conclude that the NSPD curve for *o*-H_2 is a mirror image of that for the substrate. This is a clear evidence that both species are polarized in the same coherent spin mixing process, occurring at a specific LAC.

However, when we look not only at the shape of the NSPD curves but also on the magnitude of the polarization, we clearly see that NMR signals of Ir-HH and free H_2 are considerably weaker than those of fPy (compare NMR signal intensities in Figs. 2 and 3). At the same time, the NMR enhancements are comparable for Py and both forms of H_2 because the thermal signals of the H_2 species are also much weaker due to the much lower concentration of H_2 as compared to Py.

Our analysis predicts that after spin order transfer in the SABRE complex the resulting net polarization, which is the sum of the polarizations of H_2 and the substrate, must be zero. Consequently, polarization of Py (in the free and bound forms) and of H_2 (also in the free and bound forms) is expected to be equal in amplitude. The lower amplitude of polarization of the H_2 species is due to the fact that (i) some fraction of the dissolved H_2 molecules leaves the solution and (ii) the T_1-relaxation times of the Ir-HH and H_2 protons are about 1–2 s (as measured by the inversion-recovery experiment), whereas the T_1-relaxation time of Py in complex and in bulk are about 5 s and 30 s. This results in faster loss of polarization for H_2 and Ir-HH. As a consequence, the resulting NMR signals of Py are stronger than those of Ir-HH and H_2.

The final point that we would like to address in this subsection is concerning SABRE experiments with low spectral resolution: this situation is met in low-field NMR experiments or in the presence of strong field gradients used in MRI. Previous observation of strong NMR enhancements in low-field SABRE studies [4,7,37] was explained by the strong difference in T_1-relaxation times of a substrate and the H_2 species. Our high-resolution studies show that this is a valid assumption: polarization of *o*-H_2 is subject to fast relaxation so that as a consequence net polarization is formed.

5.3. High-field SABRE effect

As has been found earlier and confirmed by our experiments, high-field SABRE is also feasible and occurs presumably *via* cross-relaxation. However, high-field polarization transfer is much less efficient as compared to low-field transfer by coherent mixing. Nonetheless, high-field SABRE can be used to study molecular dynamics of SABRE complexes (where the cross-relaxation occurs) and to enhance NMR signals [46] avoiding the field-cycling step. For improving the performance of high-field SABRE it is important to model polarization transfer by cross-relaxation in SABRE complexes on a quantitative level or to design molecular systems, where LAC conditions are fulfilled at higher magnetic fields. An alternative approach is to mimic LAC conditions by applying resonant RF-fields with properly set parameters. The idea of this technique [47,48] follows from the concept that LACs play a key role in efficient SABRE formation.

6. Conclusions

Our results provide strong evidence that (i) at low fields the dominant polarization transfer mechanism is coherent spin mixing and that (ii) this mixing is most efficient at LAC regions. It appears that the LAC-based approach to SABRE is valid for all systems, for which the polarization dispersion has been measured. The idea that LACs play a key role in the spin dynamics in SABRE experiments is further supported by comparison of the results for complexes with and without a ^{31}P atom: the presence of spin–spin interactions of protons with the phosphorus spin splits the LACs and doubles the number of features in the SABRE NSPD curve. Altogether, we can conclude that LACs give a clear and relatively simple description of the complex spin dynamics in SABRE experiments and grasp its main peculiarities such as unimodal (for the Imes catalyst) or bimodal (for Crabtree's catalyst) polarization dispersion of the SABRE effect. It also explains the similarity of SABRE NSPD curves for a variety of different substrates.[44] In addition, the LAC analysis provides important information about the structure of the SABRE complexes: here we demonstrated that the coupling between the Ir-HH protons is negative, corresponding to the dihydride.

An interesting observation is that SABRE also enables to polarize the H_2 molecule bound to the complex and in its free form in the solution; polarization of H_2 is always opposite to that of the substrate additionally supporting our LAC analysis. H_2 bound to the SABRE complex is the primarily polarized species, whereas polarized H_2 in solution results from exchange between bound and free H_2. Polarization of H_2 and Ir-HH has not been analyzed in detail before. The opposite sign of polarization of both hydrogen species (with respect to that of the substrate) is a direct consequence of coherent spin mixing at LACs. Thus, substrate polarization formation is always accompanied by the *para*-to-*ortho* conversion in Ir-HH.

It is worth noting that the idea that LACs govern the spin dynamics in SABRE experiments can be utilized in other experimental schemes as well. Recently, it was demonstrated that conditions for having LACs at high magnetic fields can be fulfilled by introducing RF-fields with carefully set amplitude and frequency [47,48]. This enables efficient spin order transfer between *p*-H_2 and the substrate and thus SABRE at the high-field. We expect that this promising methodology can be utilized to make SABRE a high-field technique and thus to broaden considerably the range of SABRE applications.

Finally, we have reported the dispersion of the SABRE effect up to fields of 16.4 T. Our results at high field are consistent with those obtained earlier in Ref. [11]: the most likely explanation of high-field SABRE is polarization transfer in the complex due to cross-relaxation. Although the NMR enhancements are much lower than those achieved by spin mixing at low fields the high-field SABRE effect can be useful for certain NMR applications [46].

An interesting direction to go further is studying polarization transfer to spin-1/2 hetero-nuclei, such as ^{13}C, ^{15}N and ^{31}P. The feasibility of such transfer has already been demonstrated [1,7,41,49,50]. Now, with the knowledge about the role of LACs in the formation of SABRE one can further increase the performance of the polarization transfer stage in such experiments and optimize the resulting SABRE-derived enhancements for spin-1/2 hetero-nuclei.

Acknowledgments

This work was supported by the Russian Science Foundation (Grant No. 14-13-01053). H.-M.V. acknowledges the Alexander von Humboldt Foundation.

Appendix A. Supplementary material

Supplementary data associated with this article contains: NMR spectra of SABRE complexes; TOCSY spectra; EXSY spectra; high-field SABRE spectra; NMR parameters of SABRE complexes used in simulations. It can be found, in the online version, at http://dx.doi.org/10.1016/j.jmr.2015.10.006.

References

[1] R.W. Adams, J.A. Aguilar, K.D. Atkinson, M.J. Cowley, P.I.P. Elliott, S.B. Duckett, G.G.R. Green, I.G. Khazal, J. López-Serrano, D.C. Williamson, Reversible interactions with para-hydrogen enhance NMR sensitivity by polarization transfer, Science 323 (2009) 1708–1711.

[2] R.H. Crabtree, H. Felkin, T. Fillebeen-Khan, G.E. Morris, Dihydridoiridium diolefin complexes as intermediates in homogeneous hydrogenation, J. Organomet. Chem. 168 (1979) 183–195.

[3] H. Zeng, J. Xu, M.T. McMahon, J.A.B. Lohman, P.C.M. van Zijl, Achieving 1% NMR polarization in water in less than 1 min using SABRE, J. Magn. Reson. 246 (2014) 119–121.

[4] J.-B. Hövener, N. Schwaderlapp, T. Lickert, S.B. Duckett, R.E. Mewis, L.A.R. Highton, S.M. Kenny, G.G.R. Green, D. Leibfritz, J.G. Korvink, J. Hennig, D. von Elverfeldt, A hyperpolarized equilibrium for magnetic resonance, Nat. Commun. 4 (2013) 2946.

[5] N. Eshuis, N. Hermkens, B.J.A. van Weerdenburg, M.C. Feiters, F.P.J.T. Rutjes, S.S. Wijmenga, M. Tessari, Toward nanomolar detection by NMR through SABRE hyperpolarization, J. Am. Chem. Soc. 136 (2014) 2695–2698.

[6] N. Eshuis, B.J.A. van Weerdenburg, M.C. Feiters, F.P.J.T. Rutjes, S.S. Wijmenga, M. Tessari, Quantitative trace analysis of complex mixtures using SABRE hyperpolarization, Angew. Chem., Int. Ed. 54 (2015) 1481–1484.

[7] J.-B. Hövener, N. Schwaderlapp, R. Borowiak, T. Lickert, S.B. Duckett, R.E. Mewis, R.W. Adams, M.J. Burns, L.A.R. Highton, G.G.R. Green, A. Olaru, J. Hennig, D. von Elverfeldt, Toward biocompatible nuclear hyperpolarization using signal amplification by reversible exchange: quantitative *in situ* spectroscopy and high-field imaging, Anal. Chem. 86 (2014) 1767–1774.

[8] A.S. Kiryutin, K.L. Ivanov, A.V. Yurkovskaya, R. Kaptein, H.-M. Vieth, Transfer of parahydrogen induced polarization in scalar coupled systems at variable magnetic field, Z. Phys. Chem. 226 (2012) 1343–1362.

[9] S. Grosse, F. Gubaydullin, H. Scheelken, H.-M. Vieth, A.V. Yurkovskaya, Field cycling by fast NMR probe transfer: design and application in field-dependent CIDNP experiments, Appl. Magn. Reson. 17 (1999) 211–225.

[10] A.N. Pravdivtsev, A.V. Yurkovskaya, H.-M. Vieth, K.L. Ivanov, R. Kaptein, Level anti-crossings are a key factor for understanding para-hydrogen-induced hyperpolarization in SABRE experiments, ChemPhysChem 14 (2013) 3327–3331.

[11] D.A. Barskiy, K.V. Kovtunov, I.V. Koptyug, P. He, K.A. Groome, Q.A. Best, F. Shi, B. M. Goodson, R.V. Shchepin, A.M. Coffey, K.W. Waddell, E.Y. Chekmenev, The feasibility of formation and kinetics of NMR signal amplification by reversible exchange (SABRE) at high magnetic field (9.4 T), J. Am. Chem. Soc. 136 (2014) 3322–3325.

[12] M. Fekete, O. Bayfield, S.B. Duckett, S. Hart, R.E. Mewis, N. Pridmore, P.J. Rayner, A. Whitwood, Iridium(III) Hydrido N-heterocyclic carbene–phosphine complexes as catalysts in magnetization transfer reactions, Inorg. Chem. 52 (2013) 13453–13461.

[13] S. Gründemann, H.H. Limbach, G. Buntkowsky, S. Sabo-Etienne, B. Chaudret, Distance and scalar HH-coupling correlations in transition metal dihydrides and dihydrogen complexes, J. Phys. Chem. A 103 (1999) 4752–4754.

[14] G. Buntkowsky, J. Bargon, H.H. Limbach, A dynamic model of reaction pathway effects on parahydrogen-induced nuclear spin polarization, J. Am. Chem. Soc. 118 (1996) 8677–8683.

[15] J. Matthes, T. Pery, S. Gründemann, G. Buntkowsky, S. Sabo-Etienne, B. Chaudret, H.H. Limbach, Bridging the gap between homogeneous and heterogeneous catalysis: ortho/para-H_2 conversion, hydrogen isotope scrambling and hydrogenation of olefins by $Ir(CO)Cl(PPh_3)_2$, J. Am. Chem. Soc. 126 (2004) 8366–8367.

[16] J. Matthes, S. Gründemann, G. Buntkowsky, B. Chaudret, H.H. Limbach, NMR studies of the reaction path of the catalyzed ortho-para-H_2 conversion in solid benzene, Appl. Magn. Reson. 44 (2013) 247–265.

[17] G. Buntkowsky, B. Walaszek, A. Adamczyk, Y. Xu, H.H. Limbach, B. Chaudret, Mechanism of nuclear spin initiated para-H_2/ortho-H_2 conversion, Phys. Chem. Chem. Phys. 8 (2006) 1929–1935.

[18] M.J. Cowley, R.W. Adams, K.D. Atkinson, M.C.R. Cockett, S.B. Duckett, G.G.R. Green, J.A.B. Lohman, R. Kerssebaum, D. Kilgour, R.E. Mewis, Iridium N-heterocyclic carbene complexes as efficient catalysts for magnetization transfer from para-hydrogen, J. Am. Chem. Soc. 133 (2011) 6134–6137.

[19] L.D. Vazquez-Serrano, B.T. Owens, J.M. Buriak, The search for new hydrogenation catalyst motifs based on N-heterocyclic carbene ligands, Inorg. Chim. Acta 359 (2006) 2789–2797.

[20] K.D. Atkinson, M.J. Cowley, P.I.P. Elliott, S.B. Duckett, G.G.R. Green, J. López-Serrano, A.C. Whitwood, Spontaneous transfer of parahydrogen derived spin order to pyridine at low magnetic field, J. Am. Chem. Soc. 131 (2009) 13362–13368.

[21] R.H. Crabtree, H. Felkin, G.E. Morris, Cationic iridium diolefin complexes as alkene hydrogenation catalysts and the isolation of some related hydrido complexes, J. Organomet. Chem. 141 (1977) 205–215.

[22] R.H. Crabtree, Iridium compounds in catalysis, Acc. Chem. Res. 12 (1979) 331–337.

[23] R.H. Crabtree, G.E. Morris, Some diolefin complexes of iridium(I) and a trans-influence series for the complexes [IrCl(cod)L], J. Organomet. Chem. 135 (1977) 395–403.

[24] I. Kownacki, M. Kubicki, K. Szubert, B. Marciniec, Synthesis, structure and catalytic activity of the first iridium(I) siloxide versus chloride complexes with 1,3-mesitylimidazolin-2-ylidene ligand, J. Organomet. Chem. 693 (2008) 321–328.

[25] L. Braunschweiler, R.R. Ernst, Coherence transfer by isotropic mixing: application to proton correlation spectroscopy, J. Magn. Reson. 53 (1983) 521–528.

[26] J. Keeler, Understanding NMR Spectroscopy, second ed., John Wiley & Sons, UK, 2010.

[27] L. Buljubasich, M.B. Franzoni, H.W. Spiess, K. Münnemann, Level anti-crossings in parahydrogen induced polarization experiments with Cs-symmetric molecules, J. Magn. Reson. 219 (2012) 33–40.

[28] M.B. Franzoni, L. Buljubasich, H.W. Spiess, K. Münnemann, Long-lived ^{1}H singlet spin states originating from para-hydrogen in Cs-symmetric molecules stored for minutes in high magnetic fields, J. Am. Chem. Soc. 134 (2012) 10393–10396.

[29] D.H. Jones, J.A. Labinger, D.P. Weitekamp, Anomalous scalar couplings in trihydrides and quantum mechanical exchange, J. Am. Chem. Soc. 111 (1989) 3087–3088.

[30] K.W. Zilm, D.M. Heinekey, J.M. Millar, N.G. Payne, P. Demou, Proton–proton exchange couplings in transition-metal polyhydrides, J. Am. Chem. Soc. 111 (1989) 3088–3089.

[31] H.H. Limbach, S. Ulrich, S. Gründemann, G. Buntkowsky, S. Sabo-Etienne, B. Chaudret, G.J. Kubas, J. Eckert, NMR and INS line shapes of transition metal hydrides in the presence of coherent and incoherent dihydrogen exchange, J. Am. Chem. Soc. 120 (1998) 7929–7943.

[32] H.H. Limbach, G. Scherer, M. Maurer, B. Chaudret, On the mechanism of coherent dihydrogen tunneling in transition-metal trihydrides, Angew. Chem. Intl. Ed. 31 (1992) 1369–1372.

[33] J.W. Emsley, J. Feeney, L.H. Sutcliffe, High Resolution Nuclear Magnetic Resonance Spectroscopy, Pergamon Press, London, 1965.

[34] K.L. Ivanov, A.V. Yurkovskaya, H.-M. Vieth, Analytical solutions for parahydrogen induced polarization, Z. Phys. Chem. 236 (2012) 1315–1342.

[35] T. Theis, M.P. Ledbetter, G. Kervern, J.W. Blanchard, P.J. Ganssle, M.C. Butler, H. D. Shin, D. Budker, A. Pines, Zero-field NMR enhanced by parahydrogen in reversible exchange, J. Am. Chem. Soc. 134 (2012) 3987–3990.

[36] R.W. Adams, S.B. Duckett, R.A. Green, D.C. Williamson, G.G.R. Green, A theoretical basis for spontaneous polarization transfer in non-hydrogenative parahydrogen-induced polarization, J. Chem. Phys. 131 (2009) 194505.

[37] J.-B. Hövener, S. Knecht, N. Schwaderlapp, J. Hennig, D. von Elverfeldt, Continuous re-hyperpolarization of nuclear spins using parahydrogen: theory and experiment, ChemPhysChem 15 (2014) 2636.

[38] S. Alexander, Fast-exchange width of nuclear magnetic resonance spectra, J. Chem. Phys. 40 (1963) 1787–1788.

[39] G.J. Binsch, A unified theory of exchange effects on nuclear magnetic resonance line shapes, Am. Chem. Soc. 91 (1969) 1304–1309.

[40] S. Glöggler, R. Müller, J. Colell, M. Emondts, M. Dabrowski, B. Blumich, S. Appelt, Para-hydrogen induced polarization of amino acids, peptides and deuterium-hydrogen gas, Phys. Chem. Chem. Phys. 13 (2011) 13759–13764.

[41] V.V. Zhivonitko, I.V. Skovpin, I.V. Koptyug, Strong ^{31}P nuclear spin hyperpolarization produced via reversible chemical interaction with parahydrogen, Chem. Commun. 51 (2015) 2506–2509.

[42] K.L. Ivanov, A.N. Pravdivtsev, A.V. Yurkovskaya, H.-M. Vieth, R. Kaptein, The role of level anti-crossings in nuclear spin hyperpolarization, Prog. Nucl. Magn. Reson. Spectr. 81 (2014) 1.

[43] S.E. Korchak, K.L. Ivanov, A.V. Yurkovskaya, H.-M. Vieth, Para-hydrogen induced polarization in multi-spin systems studied at variable magnetic field, Phys. Chem. Chem. Phys. 11 (2009) 11146.

[44] E.B. Dücker, L.T. Kuhn, K. Münnemann, C. Griesinger, Similarity of SABRE field dependence in chemically different substrates, J. Magn. Reson. 214 (2012) 159–165.

[45] H. Zeng, J. Xu, J. Gillen, M.T. McMahon, D. Artemov, J.-M. Tyburn, J.A.B. Lohman, R.E. Mewis, K.D. Atkinson, G.G.R. Green, S.B. Duckett, P.C.M. Van Zijl, Optimization of SABRE for polarization of the tuberculosis drugs pyrazinamide and isoniazid, J. Magn. Reson. 237 (2013) 73–78.

[46] M.L. Truong, F. Shi, P. He, B. Yuan, K.N. Plunkett, A.M. Coffey, R.V. Shchepin, D. A. Barskiy, K.V. Kovtunov, I.V. Koptyug, K.W. Waddell, B.M. Goodson, E.Y. Chekmenev, Irreversible catalyst activation enables hyperpolarization and water solubility for NMR signal amplification by reversible exchange, J. Phys. Chem. B 118 (2014) 13882–13889.

[47] A.N. Pravdivtsev, A.V. Yurkovskaya, H.-M. Vieth, K.L. Ivanov, Spin mixing at level anti-crossings in the rotating frame makes high-field SABRE feasible, Phys. Chem. Chem. Phys. 16 (2014) 24672–24675.

[48] T. Theis, M. Truong, A.M. Coffey, E.Y. Chekmenev, W.S. Warren, LIGHT-SABRE enables efficient in-magnet catalytic hyperpolarization, J. Magn. Reson. 248 (2014) 23–26.
[49] T. Theis, M.L. Truong, A.M. Coffey, R.V. Shchepin, K.W. Waddell, F. Shi, B.M. Goodson, W.S. Warren, E.Y. Chekmenev, Microtesla SABRE enables 10% nitrogen-15 nuclear spin polarization, J. Am. Chem. Soc. 137 (2015) 1404–1407.
[50] A.N. Pravdivtsev, A.V. Yurkovskaya, H. Zimmermann, H.-M. Vieth, K.L. Ivanov, Transfer of SABRE-derived hyperpolarization to spin ½ heteronuclei, RSC Adv. 5 (2015) 63615–63623.